1 September 1999

ELSEVIER

Optics Communications 168 (1999) 195–200

OPTICS COMMUNICATIONS

www.elsevier.com/locate/optcom

Frequency tracking and stabilization of a tunable dual-wavelength external-cavity diode laser

L. Hsu *, L.C. Chi, S.C. Wang, Ci-Ling Pan

Institute of Electro-Optical Engineering and Department of Electrophysics, National Chiao Tung University, Hsinchu 30010, Taiwan

Received 8 April 1999; received in revised form 24 June 1999; accepted 29 June 1999

Abstract

We show a unique dual-wavelength external-cavity laser diode with frequency tracking capability and obtain a stable beat frequency between the dual-wavelength output. By using a Fabry–Perot interferometer as the frequency discriminator and the time-gating technique in a servo loop, the peak-to-peak frequency fluctuations were stabilized, with respect to the Fabry–Perot cavity, to 86 kHz in the dual-wavelength output at 802.5 and 804.5 nm, and to 17 kHz in their 0.9 THz beat signal. Similar performance was achieved for tuning of the dual wavelength separation ranging from 0.2 to 4 nm. © 1999 Published by Elsevier Science B.V. All rights reserved.

PACS: 40.60.P
Keywords: Dual-wavelength external-cavity semiconductor laser; Time gating; Frequency tracking; Frequency stabilization; Terahertz beat frequency

1. Introduction

Tunable external cavity semiconductor lasers (ECL) [1] are important for an array of applications such as wavelength-division-multiplexed (WDM) optical communication, high-resolution spectroscopy and optical metrology. Frequency control of such lasers is often mandatory in practice [2]. On the other hand, an ECL capable of generating multiple wavelengths is also desirable. An example of such lasers is the tunable continuous wave dual-wavelength external-cavity laser (2-λ-ECL) as we demonstrated earlier [3,4]. The coaxial output of the two modes of the 2-λ-ECL produces an intensity-modulated signal at frequencies tunable beyond 7 THz [5]. This characteristic is ideal for applications such as the generation of terahertz signal by optical heterodyne conversion or photomixing [6–8], for which the two laser modes should be frequency-locked and stabilized. We have demonstrated stabilization of the output of a 2-λ-ECL by locking one of the laser modes to a passive reference cavity [9]. A peak-to-peak frequency fluctuation of 4.2 MHz corresponding to a frequency stability of 1.14×10^{-8} was achieved. It is, however, not possible to determine whether the two modes fluctuate in frequency independently or in unison. In this paper, we show for the first time simultaneous frequency-tracking and stabilization of a tunable 2-λ-ECL.

* Corresponding author. Fax: +886-3-572-5230; e-mail: c2654@ms19.hinet.net

PII: S0030-4018(99)00360-0

2. Theory

The frequency tracking and stabilization of the dual-wavelength laser are realized because the two laser modes are coaxial. Consider two cavity-modes coaxial all over the cavity. The oscillating frequencies of the two cavity modes can be expressed by $\nu_1 = p\ c/2L$ and $\nu_2 = q\ c/2L$, where p and q are two integers, c is the speed of light in vacuum, and L is the overall optical-path-length of the folded external cavity. Differentiating ν_1 and ν_2 with respect to L gives

$$\frac{\Delta\nu_1}{\nu_1} = \frac{\Delta\nu_2}{\nu_2} = \frac{\Delta\nu_2 - \Delta\nu_1}{(\nu_2 - \nu_1)} = -\frac{\Delta L}{L}. \quad (1)$$

As L varies, ν_1 and ν_2 follow up in phase. The shift $\Delta\nu_{21}$ of their beat frequency $\nu_{21} = \nu_2 - \nu_1$ is then subtractive: $\Delta\nu_{21} = \Delta\nu_2 - \Delta\nu_1$. Substituting this into Eq. (1), we have, for $\nu_1 \cong \nu_2 \gg \nu_{21}$,

$$\frac{\Delta\nu_1}{\Delta\nu_2} = \frac{\nu_1}{\nu_2} \cong 1 \quad (2)$$

and

$$\frac{\Delta\nu_{21}}{\Delta\nu_1} = \frac{\nu_{21}}{\nu_1} \ll 1 \quad (3)$$

Eq. (2) suggests the feasibility of the frequency tracking of two laser cavity modes in our dual-wavelength laser. Eq. (3) predicts that the beat frequency signal can be more stable than either cavity mode.

On the other hand, in the case of conventional heterodyne conversion involving two independent laser cavities, the fluctuations of ν_1 and ν_2 are random. The variation of the corresponding beat frequency becomes statistically additive: $\Delta\nu_{21}^2 = \Delta\nu_2^2 + \Delta\nu_1^2$. In other words, the beat signal of two independent lasers is less stable than that of a single 2-λ-ECL.

3. Experimental

Fig. 1 illustrates the configuration of the tunable 2-λ-ECL and the experimental set-up. The external-cavity diode laser consisted of a laser chip, an objective lens, a grating, a lens, and a V-shaped end mirror. A broad area laser chip (SDL-2430-C) with a nominal wavelength $\lambda_o = 803.5$ nm was used as the gain medium. The laser chip has an anti-reflection (AR) coated front facet with a reflectivity of $R_1 \approx 5\%$ and high-reflection (HR) coated rear facet with $R_2 \approx 95\%$, resulting in a threshold current of 250 mA. The diverging beam of the laser from the front facet was collimated by an objective lens with a focal length of 4.5 mm and NA = 0.47, then incident on a 45 mm × 10 mm grating (1800 grooves/mm) at an angle of 75°. The first-order reflection of the grating at an angle of 29° was focused on the V-shaped gold-coated end mirror by an AR-coated lens with focal length of $f = 250$ mm, as depicted in the inset of Fig. 1. The angle of the V-shaped stripes was approximately 15°, and each stripe has a width of 130 μm. The grating-lens-stripe mirror combination corresponds to an equivalent spectral filter of 0.25 nm. The external cavity reduced the threshold current to $I_{th} = 230$ mA at λ_o. At an operating current of 1.2 I_{th}, the laser output power was about 10 mW. As a result, the spectral separation of the two output wavelengths, $\lambda_{21} = \lambda_1 - \lambda_2$, could be tuned by translating the V-shaped end mirror vertically out of or into the plane of Fig. 1. Note that the two modes are coaxial inside the laser cavity except for a small portion near the two foci on the V-shaped end mirror. This makes frequency-tracked operation possible. The zeroth-order reflection of the grating provided the coaxial dual-wavelength output. The output beam was split twice by two beam splitters. The split beams were separately directed into a power meter, a spectrum analyzer (Anritzu MS9030A), and a Fabry–Perot

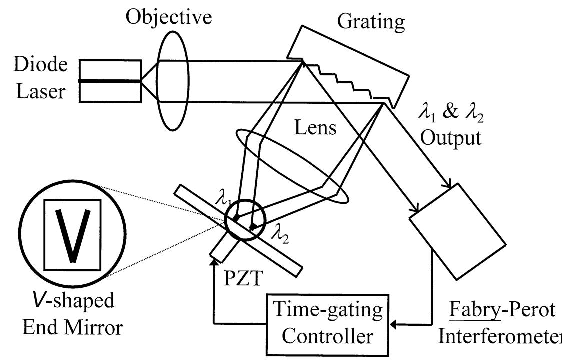

Fig. 1. The laser configuration and experimental set-up. PZT: piezoelectric transducer.

interferometer (Tech-Optics SA-2 with a free spectral range $\nu_{FSR} = 2$ GHz and finesse of 22) for frequency stabilization and measurement.

For measurement of frequency stabilization of the 2-λ-ECL, we employed the time-gating technique [10] previously developed by us for a set of laser diodes. Because the laser is dominated by the external-cavity modes with little influence by the laser chip's own modes for operating current $I \leq 1.2\ I_{th}$, the time-gating technique is applicable only on the external-cavity modes in this experiment. The basic principle of the time-gating technique is illustrated in Fig. 2. A triangular waveform voltage is used to scan the Fabry–Perot interferometer at a scanning rate of 400 Hz, as shown in Fig. 2(a). The amplitude of the scanning waveform is adjusted such that half of the scanning period $T/2$ covers one free spectral range ν_{FSR} of the Fabry–Perot interferometer. This allows the two laser frequencies ν_1 and ν_2 to appear twice within each period. A pair of time-gating pulses is then used to capture the two ν_1 signals per period, as shown in Fig. 2(b). Since the laser signals at ν_1 and ν_2 have a linewidth limited by the Fabry–Perot interferometer to about 90 MHz, thus the gating pulse width is typically adopted to only twice the width of the laser signals, which is about hundreds of megahertz, to prevent capturing the adjacent laser signals. As frequency ν_1 shifts, the duration between the two captured signals changes. It should be pointed out that the duration τ_1 is measured as the separation in time between the two peaks of the captured ν_1 signals, which is extracted from the center zeros of the first derivatives with respect to time. Therefore, the duration is relatively accurate and independent of the Fabry–Perot bandwidth.

In practice, the duration τ_1 between the peaks of the two captured ν_1 signals is then converted into a voltage signal $V_1 = k\tau_1$, where k is a constant. Similarly, the duration τ_2 between the peaks of the two captured signals of ν_2, as shown in Fig. 2(c), is converted into V_2. Consequently, for any fluctuations in laser frequency ν_1 and ν_2, the voltage signal V_i will vary according to $\Delta\nu_i = (\Delta V_i/k) \cdot (\nu_{FSR}/T)$, where $\Delta\nu_i$ and ΔV_i are the fluctuations in ν_i and V_i, respectively, for $i = 1$ and 2. We also measure a third voltage signal $V_{21} = k\tau_{21}$, which provides information on fluctuations in the difference frequency $\nu_{21} = \nu_2 - \nu_1$ according to the relationship $\Delta\nu_{21} = (\Delta V_{21}/k) \cdot (2\nu_{FSR}/T)$. Here τ_{21} is the duration between the peaks of the captured signals ν_1 and ν_2 within the same half-periods, as shown in Fig. 2(d). Either V_1 or V_2 was then sent into a proportional-integral-differential (PID) controller. The output of the PID controller is used to drive a piezo-electric transducer (PZT) mounted behind the V-shaped end mirror for laser frequency stabilization of one cavity mode.

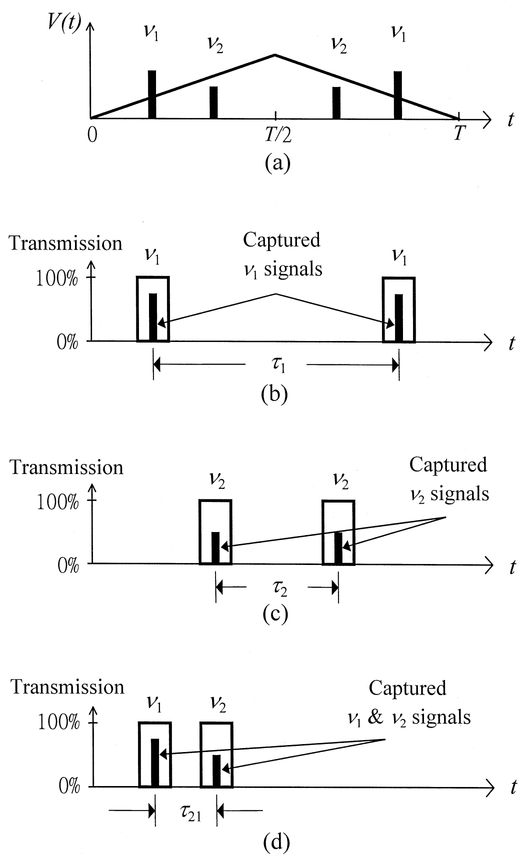

Fig. 2. Operating principle of time-gating technique. (a) scanning waveform and two laser-mode signals; (b) a pair of time-gating pulses for τ_1; (c) a pair of time-gating pulses for τ_2; (d) a pair of time-gating pulses for τ_{21}.

4. Results

The frequency tracking capability and stability of the laser modes was obtained by converting the three fluctuating voltage signals ΔV_1, ΔV_2 and ΔV_{21} into

$\Delta\nu_1$, $\Delta\nu_2$ and $\Delta\nu_{21}$ as given above. It should be noted that all the frequency fluctuations thus measured were referenced with respect to the Fabry–Perot interferometer, which is reasonably stable dur-

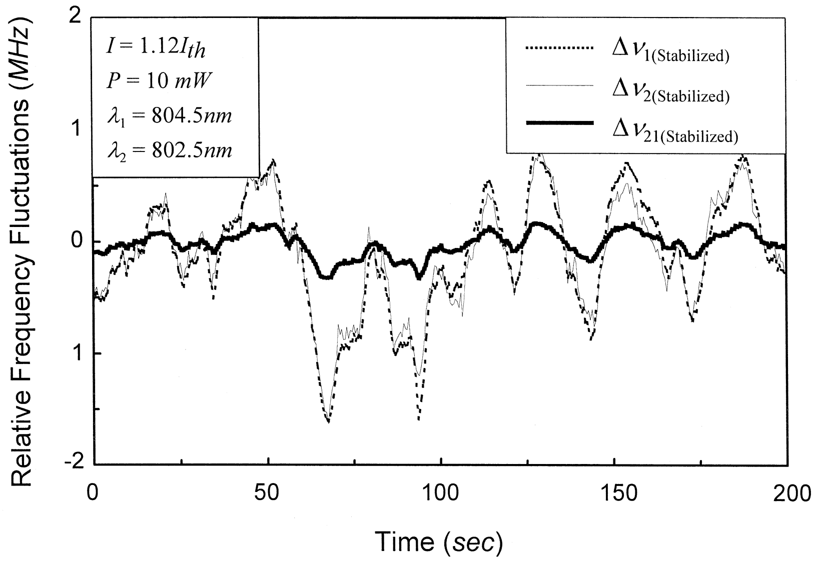

(a)

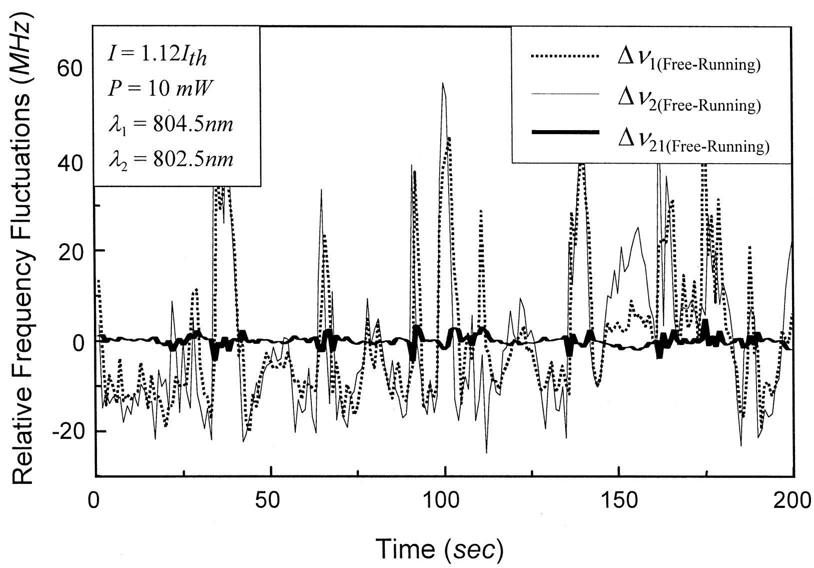

(b)

Fig. 3. (a) Relative frequency fluctuations as a function of time for $\Delta\nu_1$, $\Delta\nu_2$, and $\Delta\nu_{21}$ with stabilization ($\lambda_1 = 804.5$ nm and $\lambda_2 = 802.5$ nm); (b) relative frequency fluctuations as a function of time for $\Delta\nu_1$, $\Delta\nu_2$, and $\Delta\nu_{21}$ without stabilization ($\lambda_1 = 804.5$ nm and $\lambda_2 = 802.5$ nm).

ing the measurement period. Hence, the measured frequency stabilities of ν_1, ν_2 and ν_{21} are relative frequency stabilities. At an operating current of 1.2 I_{th}, Fig. 3(a) shows the converted $\Delta\nu_1$, $\Delta\nu_2$, and $\Delta\nu_{21}$, under stabilized conditions, as a function of time during a 200 s scan with a sampling interval of 0.5 s. The wavelengths $\lambda_1 = 804.5$ nm and $\lambda_2 = 802.5$ nm of the two oscillating modes were directly determined from the spectrum analyzer with a resolution of 0.1 nm. The side mode suppression ratio (SMSR) of the laser output was better than 10 dB. For comparison, Fig. 3(b) shows the same signals for laser without stabilization. As can be seen from the results, the peak-to-peak fluctuations are 2 MHz with stabilization and 80 MHz without stabilization. The two fluctuation signals $\Delta\nu_1$ of λ_1 and $\Delta\nu_2$ of λ_2 were nearly the same and synchronous, indicating fairly good tracking of the two oscillating wavelengths. With stabilization, the square root of the Allan variances [11] for the two modes is $\langle\Delta\nu_1\rangle \cong \langle\Delta\nu_2\rangle = 86$ kHz, corresponding to a relative frequency stability of $\langle\Delta\nu_1\rangle/\nu_1 \cong \langle\Delta\nu_2\rangle/\nu_2 = 2.3 \times 10^{-10}$. As for the beat signal at $\nu_{21} = 0.93$ THz, the fluctuation is relatively small. The square root of the Allan variances of ν_{21} is $\langle\Delta\nu_{21}\rangle = 17$ kHz. In addition, we also measured $\langle\Delta\nu_{21}\rangle$ at a fixed total output power as a function of the separation of the two wavelengths, $\lambda_{21} = \lambda_1 - \lambda_2$, for a tuning range of 0.2 nm $\leq \lambda_{21} \leq 4$ nm, as shown in Fig. 4. It can be seen that $\langle\Delta\nu_{21}\rangle = (17.2 \pm 0.4)$ kHz, which is nearly independent of the separation between the two wavelengths within the above tuning range.

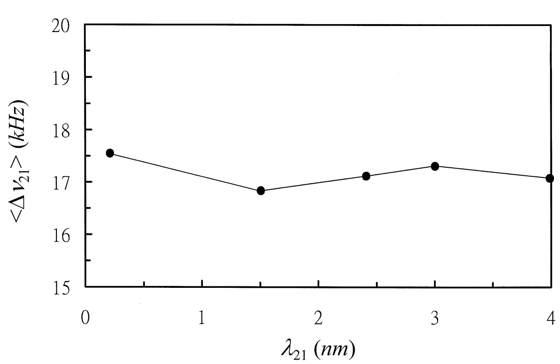

Fig. 4. Relative frequency fluctuations $\Delta\nu_{21}$ as a function of λ_{21} ($= \lambda_1 - \lambda_2$) over the range 0.2 nm $\leq \lambda_{21} \leq 4$ nm.

5. Discussion

For a perfect frequency tracking condition between the two oscillating modes, we would expect $\Delta\nu_{21}$ to be very small. However, our data shows $\Delta\nu_{21} > (\Delta\nu_2 - \Delta\nu_1)$, which suggests a slight effect of partially laser cavity dependent of the two oscillating modes ν_1 and ν_2. This may be attributed to the fact that the two coaxial modes are not perfectly coaxial within the entire cavity. In fact, the two modes do separate apart from each other within a relatively short distance between the lens and the V-shaped end mirror, as shown in Fig. 1. Denoting L_1 and L_2 as the overall optical-path-lengths of the cavities for the two modes separately, we have $\Delta\nu_1/\nu_1 = -\Delta L_1/L_1$ and $\Delta\nu_2/\nu_2 = -\Delta L_2/L_2$. Assuming that ΔL_1 and ΔL_2 fluctuate simultaneously, we may set $\Delta L_1 = \beta\Delta L_2$, where β is a constant. For $\nu_1 \cong \nu_2$, $L_1 \cong L_2$, and $\Delta\nu_{21} \cong \Delta\nu_2 - \Delta\nu_1$ in this work, we obtain $\Delta\nu_{21} = (1-\beta)\Delta\nu_2$. Substituting 17 kHz for $\Delta\nu_{21}$, 86 kHz for $\Delta\nu_2$, 3.74×10^{14} Hz for ν_2, and 75 cm for L_2 into the above expressions yields $\beta = 0.8$, $\Delta L_2 = -1.7$ Å, and $\Delta L_1 = -1.4$ Å, indicating a difference of $|\Delta L_1 - \Delta L_2| = 0.3$ Å in cavity length variation. This is reasonable since the V-shaped end mirror was mounted on the top of a moving PZT. The random fluctuations in the cavity lengths due to environmental vibration noise can be considered as the major factor in preventing the perfect frequency tracking between the two modes in the duel-wavelength laser. Furthermore, since the frequency instability induced by the cavity length fluctuations is frequency independent, this is in qualitative agreement with the plot of $\Delta\nu_{21}$ as seen in Fig. 4. We believe that the frequency tracking capability and noise reduction in the 2-λ-ECL can be improved by increasing the rigidity of the V-shaped end mirror and its mount.

6. Summary

We demonstrated the tracking capability and relative frequency stability of two coaxial oscillating modes in a dual-wavelength external-cavity laser using a time gating technique and a Fabry–Perot interferometer as the frequency discriminator. When the laser was stabilized against a reference Fabry–Perot interferometer, the peak-to-peak fluctuations of the laser frequencies were able to be stabilized to 86 kHz in the dual-wavelength output at 802.5 nm and 804.5 nm, and to 17 kHz in their 0.9 THz beat frequency signal. The frequency-tracking characteristic of the 2-λ-ECL results in a factor of five improvement in the relative frequency stability for the beat signal of the two modes. It is nearly independent of the separation between the two wavelengths for $0.2\ \text{nm} \leq (\lambda_{21} = \lambda_1 - \lambda_2) \leq 4\ \text{nm}$. With this unique frequency tracking capability, the 2-λ-ECL should be an ideal light source for applications such as heterodyning or photomixing for the generation of tunable terahertz radiation.

Acknowledgements

This work was supported in part by various grants of the National Science Council of the Republic of China.

References

[1] F.J. Durate, et al., Tunable Laser Applications, Marcel Dekker, New York, 1995.
[2] M. Ohtsu, et al., Frequency Control of Semiconductor Lasers, Wiley, New York, 1996.
[3] C.-L. Wang, C.-L. Pan, Appl. Phys. Lett. 64 (1994) 3089.
[4] C.-L. Pan, C.-L. Wang, Opt. Quantum Electron. 28 (1996) 1239.
[5] C.-L. Wang, C.-L. Pan, Opt. Lett. 20 (1995) 1292.
[6] E.R. Brown, K.A. Mcintosh, K.B. Nichols, C.L. Dennis, Appl. Phys. Lett. 66 (1995) 285.
[7] R. Paiella, K.J. Vahala, IEEE J. Quantum Electron. 32 (1996) 721.
[8] N. Onodera, Electron. Lett. 32 (1996) 1013.
[9] C.L. Pan, Y.P. Lan, S.C. Wang, CLEO'97, Tech. Digest II, Paper CWF29, 244, 1997.
[10] P.-Y. Chien, C.-L. Pan, Opt. Commun. 83 (1991) 81.
[11] D.W. Allan, Proc. IEEE 54 (1966) 221.